

## PAPER

Cite this: *Analyst*, 2021, **146**, 4615

# An enhanced fluorescence detection of a nitroaromatic compound using bacteria embedded in porous poly lactic-co-glycolic acid microbeads†

Tian Qiao,<sup>a</sup> Soohyun Kim,<sup>a</sup> Wonmok Lee <sup>\*b</sup> and Hyunjung Lee <sup>\*a</sup>

The detection of explosive nitroaromatic compounds has caused worldwide concern for human safety. In this study, we introduce a fluorescent biosensor based on porous biocompatible microspheres loaded with a bioreporter for the detection of nitroaromatic compounds. Poly(lactic-co-glycolic acid) microbeads were designed as biosensors embedded with the bacterial bioreporters. The genetically engineered bacterial bioreporter can express a green fluorescent protein in response to nitroaromatic compounds (e.g., trinitrotoluene and dinitrotoluene). The modified surface structure in microbeads provides a large surface area, as well as easy penetration, and increases the number of attached bioreporters for enhanced fluorescent signals of biosensors. Moreover, the addition of the M13 bacteriophage in open porous microbeads significantly amplified the fluorescence signal for detection by the  $\pi$ - $\pi$  interaction between peptides in the M13 bacteriophage and nitroaromatic compounds. The modification of the surface morphology, as well as the genetically engineered M13 phage, significantly amplifies the fluorescence signal, which makes the detection of explosives easier, and has great potential for the stand-off remote sensing of TNT buried in the field.

Received 24th March 2021,

Accepted 1st June 2021

DOI: 10.1039/d1an00510c

rsc.li/analyst

## 1. Introduction

The environmental problem and public security caused by nitroaromatic compounds in toxic contaminants and explosive materials raise the world's concerns. Moreover, nitro-aromatic explosives may also cause human and animal health risks through various long-term or short-term diseases (such as skin irritation, carcinogenicity, abnormal liver, anaemia and cataracts).<sup>1–3</sup> Therefore, the detection of nitroaromatic compound residuals has been urgently demanded due to the broad use of nitroaromatic compounds in the military or explosion industries.<sup>4</sup>

Satapathi and co-workers reported a poly-tryptophan/carbazole-based fluorescence resonance energy transfer (FRET) system to detect the nitroaromatic explosives.<sup>5</sup> The detection of nitroaromatic compounds was conducted by fluorescence quenching, in which FRET signals transfer from an electron-rich state to electron-deficient nitroaromatic compound molecules. Moreover, Kim and co-workers reported a highly selective and sensitive detection of nitroaromatic explosives using a

fluorescent metal-organic framework.<sup>6</sup> The synthesized Zeolitic imidazole framework-8 (ZIF-8) demonstrated a special property of colour change from ivory to red when exposed to TNT. It is possible to detect the nitroaromatic compound as low as 1 ppm with a ZIF-8-coated paper type sensor. Zargoosh and co-workers reported a technique for the fast detection of nitroaromatic explosives using the SmCrO<sub>3</sub> nanopowder in polar solvents.<sup>7</sup> It was confirmed that the quenching effect of the nitro explosives on the fluorescence signal of the SmCrO<sub>3</sub> nanopowder could come from the FRET mechanism. As for trinitrophenol, a detection limit as low as  $9.6 \times 10^{-7}$  M can be achieved in tetrahydrofuran solution.

Typical detection of the nitroaromatic compound has been performed with the cooperation of expensive gas chromatography coupled to a mass spectrometer,<sup>8</sup> ion mobility spectrometry,<sup>9</sup> and neutron activation analysis,<sup>10</sup> which are usually time-consuming and inconvenient for portable or easy use, and are not suitable for the detection of the nitroaromatic compound spread out in the field or our everyday environment.<sup>11</sup> Miniaturization, low-cost detection equipment and easy handling in outdoor field ground will become essential parameters for the detection of nitroaromatic compounds. So, it is of vital significance to develop chemicals or biosensors for nitroaromatic compound detection.<sup>12–14</sup> Compared with conventional methods, optical sensors have shown promising results, such as improved selectivity and sensitivity, low cost

<sup>a</sup>Department of Materials Science and Engineering, Kookmin Univ.77 Jeongneung-ro, Seongbuk-guSeoul, 02707, Republic of Korea. E-mail: hyunjung@kookmin.ac.kr

<sup>b</sup>Department of Chemistry, Sejong Univ., Neungdong-ro 209, Gwangjin-guSeoul, 143747, Republic of Korea. E-mail: Wonmoklee@sejong.ac.kr

†Electronic supplementary information (ESI) available: Fig. S1–S6. See DOI: 10.1039/d1an00510c

and simple equipment requirements, among various detection techniques. Therefore, in explosives detection, colorimetric or fluorescent response sensors are now becoming more and more urgently required. However, detection based on fluorescence technology is more advantageous than the detection based on absorbance because the sensitivity of fluorescence based detection is around 1000 times larger than absorbance based detection with a wider linear range.<sup>15</sup> Moreover, the portable fluorescent device can be easily operated (with source and detector) during field explosive detection. Therefore, the fluorescence sensor has significant potential as a candidate for nitroaromatic compound detection. For example, fluorescence quenching, which is based on photo-induced electron transfer, electron exchange, resonance energy transfer, and intermolecular charge transfer, is a typical optical sensing method to detect nitroaromatic compounds by a decrease of the fluorescence intensity after charge transfer between the nitroaromatic compound and fluorophores.<sup>16</sup> Gao and co-workers reported a resonance energy transfer-amplifying fluorescence quenching at the surface of silica nanoparticles for the ultrasensitive detection of trinitrotoluene (TNT) in solution and vapour environments. With only 10  $\mu\text{L}$  of solution and a few ppb of TNT vapour in the air, it can detect as low as 1 nM TNT with the silica nanoparticle assembly silicon wafer.<sup>12</sup> Among various research studies, the fluorescence quenching technique remains a dominant method when considered in the fluorescence sensing detection of nitroaromatic compounds.<sup>16</sup>

Biosensors based on genetic engineering to provide measurable signals in response to specific chemical substances have been widely used in environmental monitoring and biomedicine.<sup>17,18</sup> The research of cell-based biosensors mainly focuses on the development of microbial biological reporters, in which genetic engineering technology is used to improve sensing capabilities by editing the gene reporter. Cell-based biosensors show the properties of being produced in mass production. Through standard cell culture, microbial cells can be easily expanded in large amounts. Even without additional nutritional support, their activity can be maintained for several days, which significantly improves the sensor's practicality. Schönherr and co-workers reported that alginate-methacrylate hydrogel beads with the *N*-acylhomoserine lactone sensing *E. coli* pLuxR-GFP (model bacteria) were considered as a biosensor for *P. aeruginosa* detection.<sup>19</sup> When exposed to *N*-(3-oxododecanoyl)homoserine lactone in the concentration range of  $1.0 \times 10^{-5}$ – $1.0 \times 10^{-7}$  mol L<sup>-1</sup>, the bacteria-encapsulated microbeads manifested up to a 13-fold increase in the fluorescence intensity as a response of the green fluorescent protein (GFP) expression to the autoinducer trigger. However, GFP-based biosensors generally suffer from the shortcomings of weak fluorescence intensity for detection. There are seldom reports on biofluorescent protein sensors that detect nitroaromatic compounds due to the enhanced fluorescence signal.

In this study, we fabricated a biocompatible and biodegradable sensor for nitroaromatic compound detection. Biosensors with porous poly (lactic-co-glycolic acid) (PLGA)

microbeads loading *E. coli* MG1655\_pPROBE-PyqjFmut-egfp+ (nitroaromatic compounds-sensitive bacteria) or *E. coli* MG BL21(DE3) pBbE7k-egfp+(green fluorescent bacteria)<sup>20–22</sup> were developed to detect the nitroaromatic compounds. Nitroaromatic compounds-sensitive bacteria were designed to express GFP in response to nitroaromatic compounds in the bioreporter system. There are two strategies for enhancing the fluorescence intensity in this study. First, the open porous biocompatible and biodegradable PLGA carriers are designed to achieve a lot of pores in their surfaces and provide a large space for bioreporter enrichment, which also results in an enhanced response signal. Second, to induce the enrichment of target chemical substances in the microbeads from the lack of environment, the M13 bacteriophage with the target-binding function was incorporated into the microbeads. The binding effect of gathering nitroaromatic compounds together by the M13 bacteriophage also makes a contribution to the increase of the fluorescence intensity. This is the first fluorescent biosensor formed by combining microspheres with a connected open porous structure, GFP-producing bacteria and nitroaromatic-binding M13 bacteriophage. This new type of sensor is inexpensive, environmentally friendly, field-deployable and conducive to mass production. Fluorescent signal-enhanced sensors demonstrate great application potential in detecting explosives without complicated precision instruments at a long distance.

## 2. Experimental section

### 2.1 Materials

PLGA (75 : 25, MW 66 000–107 000) and ammonium bicarbonate ( $\text{NH}_4\text{HCO}_3$ ), Luria Broth Miller (LB broth), phosphate buffered saline (PBS), and thiazolyl blue tetrazolium bromide (MTT) were purchased from Sigma-Aldrich, Inc., USA. Sodium hydroxide (NaOH), methylene chloride ( $\text{CH}_2\text{Cl}_2$ ) and *N,N*-dimethylformamide (DMF) were purchased from Daejung Chemicals & Metals Co., Ltd. Polyvinyl alcohol (PVA) was purchased from Junsei Chemical Co., Ltd, Japan. All chemicals were of analytical grade and used without any other purification.

Green fluorescent bacteria and nitroaromatic compounds-sensitive bacteria were applied as bioreporters.<sup>23</sup> Kanamycin was used as an antibiotic and isopropyl  $\beta$ -D-1-thiogalactopyranoside (IPTG) as an autoinducer. Among them, the genetically engineered plasmid and mutated sequence information for nitroaromatic compounds-sensitive bioreporter are described in Fig. S1.† A genetically engineered M13 bacteriophage was employed as a nitroaromatic compound-binding material received from Professor Jin-Woo Oh at Pusan National University.<sup>24</sup>

### 2.2 Preparation of porous microbeads

PLGA microspheres were prepared by the double emulsion evaporation method, as previously described.<sup>25</sup> Two mL of deionized (DI) water containing 5 wt%  $\text{NH}_4\text{HCO}_3$  was added to 7 mL of  $\text{CH}_2\text{Cl}_2$  containing 240 mg PLGA. The first water/oil ( $W_1/O$ ) emulsion was prepared using a homogenizer (IKA ULTRA-TURRAX® T 25 digital) at 12 000 rpm for 3 min. This

primary emulsion was immediately transferred into a beaker containing 150 mL of 0.1 wt% PVA solution, and then re-emulsified ( $W_1/O/W_2$ ) by using an overhead propeller for more than 4 hours at 200 rpm. After the solvent was evaporated entirely, the microbeads were separated by a standard sieve with a mesh diameter of 75  $\mu\text{m}$  and washed three times with DI water. For the hydrolysis process, a 0.2 M NaOH solution was used to treat the microbeads for 25 minutes, and then rewashed with DI water three times to remove the remaining NaOH solution. For fabrication of the non-porous microbeads, the first emulsion ( $W_1/O$ ) was not required, and the oil phase without  $W_1$  droplets was added into a 0.1 wt% PVA solution. After stirring with an overhead propeller for 4 hours, the organic solvent was perfectly evaporated, and the non-porous microbeads were harvested. The surface morphology and size of the microbeads under different operating parameters were observed *via* a scanning electron microscope (SEM, JEOL Ltd, Japan).

### 2.3 PLGA microbeads loading with bioreporters

For the bacteria adhesion experiment, green fluorescent bacteria were used as the bioreporters. A green fluorescent bacteria colony was transferred into a 50 mL centrifuge tube with 20 mL LB broth medium and 20  $\mu\text{L}$  kanamycin as an antibiotic. After culturing of the solution for 8 hours in an incubator (Vs-101Si, Vision Scientific Co., Ltd, Korea, culture condition: 37  $^\circ\text{C}$  at 200 rpm), 20  $\mu\text{L}$  IPTG as an autoinducer was added to this bacteria growth media. The concentration of the bioreporters in the solution was monitored by measuring the optical density (OD value) of the bacteria solution in a UV/Vis spectrometer (PerkinElmer) at 600 nm. After being cultured in an incubator for 18 hours, the OD value of the bacteria solution was set to be 1.0 at 600 nm by diluting with LB broth medium. Then, non-open porous microbeads or open porous microbeads were immersed into bacteria solution and after a specific time, microbeads were taken out and washed with PBS thoroughly. Bacterial embedding behaviour was monitored by fluorescence microscopy and confocal laser scanning microscopy (CLSM, Leica TCS SP5) using emitted fluorescence at 520 nm with the excitation wavelength at 485 nm by loading bioreporters.

For the nitroaromatic compound sensing experiment, the nitroaromatic compounds-sensitive bacteria were utilized as the bioreporter. In TNT/dinitrotoluene (DNT) sensing experiments, the microbeads embedded with bacteria were immersed in TNT or DNT solution for a specific time (24 hours, 48 hours, and 96 hours later). The microscopic fluorescence images were observed, and the fluorescence area in each image was chosen using Image J.<sup>26,27</sup> Area values of ten or more microbeads in each microscopic image were averaged out for quantitative fluorescence analysis. Fluorescence intensity was normalized by microbeads before sensing. The sensing experiments with the cooperation of the M13 bacteriophage were conducted with the same procedure as described above. The only different issue is that the M13 bacteriophage with various concentrations is cultured with bacteria solution

together. A multi-mode microplate reader (Synergy HTX, Biotek) was used to quantify the fluorescence intensity in a fluorescence mode with excitation at 485 nm and emission at 520 nm.

### 2.4 The bacterial embedding property in microbeads *via* MTT assay

The bacteria loading microbeads were immersed into PBS medium, and MTT solution (5 mg  $\text{mL}^{-1}$  in PBS) was added to bacteria including PBS medium (volume ratio, MTT: bacteria/PBS = 1 : 10). The mixture was incubated for 4 hours at 37  $^\circ\text{C}$ . After washing, the microbeads were immersed into the mixture of 0.2 M NaOH and DMF (volume ratio, 1 : 1) to decompose PLGA and ensure formazan crystals' total solubility. The homogenous purple solution was transferred to a 96-well plate as 200  $\mu\text{L}$  per well. The absorbance was recorded as the OD value at 570 nm, which indicates the cell viability.

## 3. Results and discussion

### 3.1 Preparation of porous microbeads

Fig. 1a illustrates the schematic diagram for the fabrication of the porous microbeads. SEM morphology of the non-open porous Fabrication condition.  $W_1$  phase: 5 wt%  $\text{NH}_4\text{HCO}_3$ ; oil

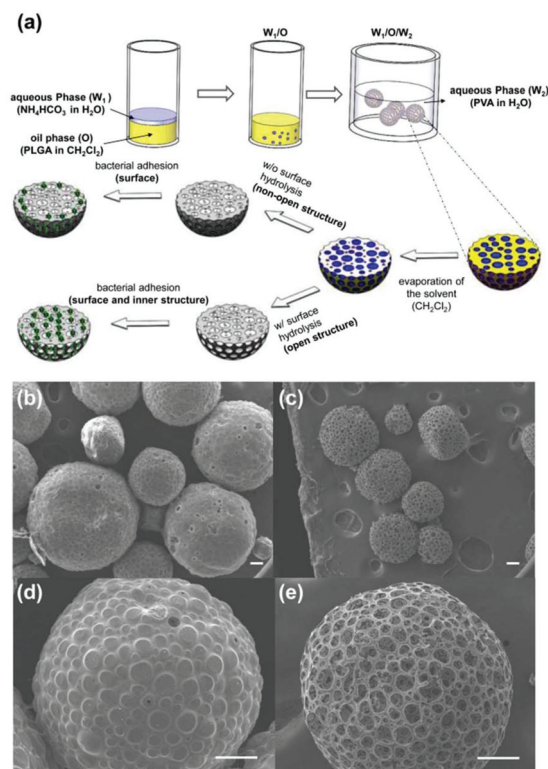


**Fig. 1** Fabrication of the bacteria embedded microbead sensor. (a) Schematic diagram of the fabrication of the bacteria encapsulated porous PLGA microbeads. SEM morphology of the microbeads (b) (d) before NaOH treatment and (c) (e) after NaOH treatment. Scale bars indicate 100  $\mu\text{m}$ .

phase: 2.5 wt% PLGA in 3.5 mL  $\text{CH}_2\text{Cl}_2$ ; W2 phase: 0.1 wt% PVA; NaOH treatment: 0.2 M for 25 min; o/w ratio = 1 : 3.5; microbeads and open porous microbeads are shown in Fig. 1b, d and c, e. The porous PLGA microbeads were fabricated by  $W_1/O/W_2$  double emulsion method by mixing  $\text{NH}_4\text{HCO}_3$  in the inner  $W_1$  droplets as a gas bubble generation agent. The oil phase was  $\text{CH}_2\text{Cl}_2$  containing PLGA. The  $W_1$  droplets, which were dispersed in the oil phase, finally were evolved into pores. The dissolved  $\text{NH}_4\text{HCO}_3$  in the  $W_1$  droplets generated gas bubbles ( $\text{NH}_3$  and  $\text{CO}_2$ ), and these gas bubbles played a significant role in supporting the emulsion stabilization since there was no additional surfactant used in the primary  $W_1/O$  emulsion. In addition, these gas bubbles were evolved into small secondary pores, which could be considered as the passages between the big pores.<sup>28,29</sup> In total, this experiment lasted at least 4 hours due to sufficient evaporation of the organic solvents. During the evaporation in the second emulsification step, the oil phase became viscous and elastic with the gradual removal of the organic solvent and solidified in the end. PLGA is a co-polymer abundant with a lot of ester bonds, and sodium hydroxide can accelerate the ester bond's hydrolysis in PLGA. The partial hydrolysis process was used to modify the surface to generate the open porous structure at the microbeads' surface.

### 3.2 The comparison of bacteria adhesion between non-open porous and open porous microbeads

Fig. 2a and b show the morphology of the inner structures of the non-porous structures and open porous microbeads by confocal laser scanning microscopy. In our case, all of the green fluorescence signals (wavelength around 520 nm) were emitted from GFP, which was located within microbeads. Little fluorescence signal from the fluorescence bacteria in Fig. 1a was detected, and the fluorescent bacteria were well embedded in the open porous microbeads in Fig. 1b. It was difficult for bacteria to penetrate the inner structure without porous structures. In addition, without the NaOH hydrolysis process, the PLGA microbeads demonstrated a relatively hydrophobic surface, which was proved to be not suitable for bacterial embedment.<sup>30–32</sup> Fig. S2a and b† illustrate the SEM morphology of the fluorescent bacteria and porous microbeads embedded with fluorescent bacteria. The black arrow indicates the skeleton of the PLGA microbead and the red arrow indicates the existence of fluorescent bacteria. As a result, the open porous structure of the PLGA microbeads demonstrated a high embedment of bacteria, and fluorescent bacteria were successfully attached with the porous microbeads. The microbead structure is known to be a significant factor in influencing the embedment of biological factors, such as bacteria.<sup>33,34</sup> Here, we gave a comparison of the different structures of microbeads to survey the property of bacterial embedment. Fig. 2c and d illustrate the morphologies of non-open porous microbeads and open porous microbeads in fluorescence mode. The microbeads were cultured in the bacterial solution for 6 hours, and the mean fluorescence intensity was measured by fluorescence microscopic image. As mentioned before, the green

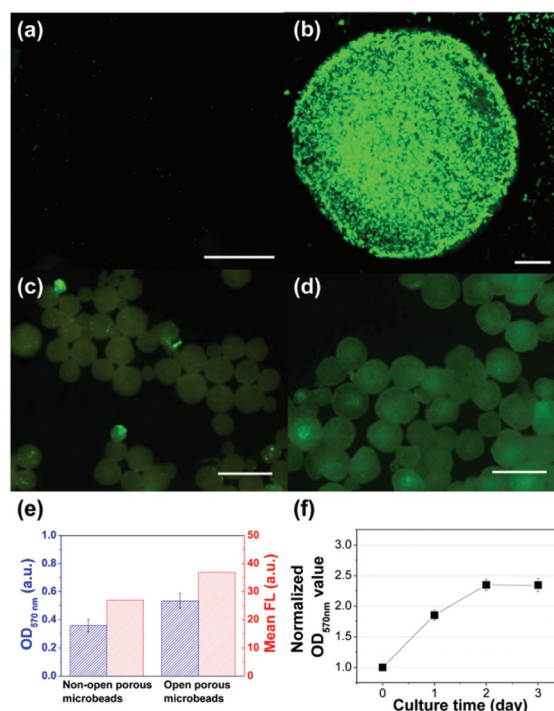


**Fig. 2** The comparison of the bacteria adhesion between the non-open porous and open porous microbeads. CLSM image of the fluorescent bacteria embedded in the non-porous microbeads (a) and open porous microbeads (b). Scale bars represent 100  $\mu\text{m}$ . Fluorescence mode OM image of the non-open porous (c) and open porous (d) PLGA microbeads loading with green fluorescent bacteria. Scale bars represent 500  $\mu\text{m}$ . (e) OD<sub>570 nm</sub> value and mean fluorescence intensity of the non-open porous and open porous microbeads. (f) The normalized OD<sub>570 nm</sub> value vs. culture time in the open porous PLGA microbeads.

fluorescence signals were from the GFP in the fluorescent bacteria. It was obvious to find that the open porous microbeads demonstrated greater fluorescence than those without an open porous structure in fluorescence mode. This hinted that a large amount of GFP was produced, and many fluorescent bacteria were embedded in the open porous structure. Quantitatively, the average values of the fluorescence intensity were obtained as 27.0 for the non-open structure and 36.8 for the open structure, as measured by microscopic fluorescence image (shown in Fig. 2e). On the one hand, the open porous microbeads provide a possibility to be embedded with more bacteria due to the large surface area.<sup>33–35</sup> The enhanced bacterial adhesion resulting from an open porous structure also was confirmed by OD value at 570 nm with MTT assay in Fig. 2e. On the other hand, to generate an open porous structure, the NaOH solution partly hydrolysed the PLGA. Meanwhile, NaOH-treated PLGA microbeads showed relatively more hydrophilic property due to the formation of some hydrophilic functional groups, such as carboxyl and hydroxyl. A lot of research studies were done to prove that the hydrophilic surface was good for the biology factor to survive.<sup>36–40</sup> As shown in Fig. 2f, the normalized OD value (570 nm) of the open porous PLGA microbeads was surveyed as a function of

the culture time. It is worth mentioning that the bioreporter's viability was still high even after 3 days, which indicates that the porous PLGA microbeads were considered a promising scaffold for bacterial adhesion. Moreover, the biodegradation behaviour of the open porous PLGA microbeads was investigated. The Fourier transform infrared spectra of the open porous PLGA microbeads before and after 14-day degradation are shown in Fig. S3a,<sup>†</sup> and the derivative of the thermogravimetric curves of the open porous PLGA microbeads before and after 14-day degradation are shown in Fig. S3b.<sup>†</sup>

### 3.3 DNT sensing performance comparison in non-open porous and open porous PLGA microbeads

The schematic diagram revealing the application of the open-porous microbeads as a nitroaromatic compound detection sensor is shown in Fig. 3a. Here, the nitroaromatic compounds-sensitive bacteria were embedded with open porous PLGA microbeads. When the nitroaromatic compounds-sensitive bacteria were activated by encountering explosive nitroaromatic compounds, especially TNT or DNT, GFP transcription initiation by PyqjF activation happened and an increase of GFP expression was activated by promoter mutation. Finally, the GFP was successfully expressed when exposed to TNT or DNT, which resulted in the enhanced green fluorescence intensity. The plasmid structure of the genetically engineered

nitroaromatic compounds-sensitive bacteria and detailed nitroaromatic compound sensing mechanism to make the GFP expressed are introduced in Fig. S1 in the ESI.<sup>†</sup> The comparison of the DNT sensing performance between the non-open porous and porous microbeads is shown in Fig. 3b. NOP\_1 indicates the non-open porous microbeads immersion in  $1 \mu\text{g mL}^{-1}$  DNT solution. OP\_100 indicates the open porous microbeads immersion in  $100 \mu\text{g mL}^{-1}$  DNT solution. The open porous PLGA microbeads showed enhanced fluorescence intensity compared to the non-open porous microbeads in both low and high concentrations of DNT solution when considering the DNT sensing performance. Notably, the sensing fluorescence intensity of OP\_1 was 2.6 folds higher than that for NOP\_1, and the sensing fluorescence intensity of OP\_100 was 3.1 folds higher than that for NOP\_100. Moreover, the pore size could be controlled during the 1<sup>st</sup> emulsion procedure. The different morphology and OD value (570 nm) of the microbeads by MTT assay with different pore sizes are shown in Fig. S4.<sup>†</sup> The group with 12 000 rpm during the 1<sup>st</sup> emulsion showed the highest bacteria adhesion ability. The inner porous structure of the porous PLGA microbeads can be proven by the CLSM images of the PLGA microbeads shown in Fig. S5.<sup>†</sup> The open porous microbeads fabricated with 12 000 rpm were considered as promising candidates for bacteria loading scaffolds of nitroaromatic compound detection.

### 3.4 DNT TNT sensing behaviour survey of porous PLGA scaffold as a function of sensing time

Fig. 4a illustrates the fluorescence intensity behaviour of the open porous PLGA microbeads embedded with nitroaromatic compounds-sensitive bacteria immersed in TNT or DNT solution for several days. The experiment and sensing mechanism are the same as those mentioned in section 3.3.

Since the fluorescence intensity in the image of 0 h is too low to distinguish clearly, the inset (at 0 h) showing the typical optical image of the porous microbeads prove the presence of some microbeads in this image. The fluorescence intensity of the porous microbeads increased with the increase of the immersion time in TNT or DNT. As time elapsed, more GFP was expressed and the intensity was gradually enhanced. The average intensity as a function of immersion time in TNT or DNT is shown in Fig. 4b and c. The normalized intensity of microbeads in the DNT group was higher than those in the TNT group. Moreover, there was no significant difference in the TNT group when the concentration of the TNT solution increased from  $10 \mu\text{g mL}^{-1}$  to  $100 \mu\text{g mL}^{-1}$ . However, after 96 hours, the normalized fluorescence intensity was enhanced by 6.5- and 14-fold in the  $10 \mu\text{g mL}^{-1}$  and  $100 \mu\text{g mL}^{-1}$  DNT solution, respectively. The durability of the fluorescence signal from this functioning microbead sensor could be maintained even after 96 hours.

### 3.5 Enhanced fluorescence intensity of DNT sensing performance by M13 bacteriophage

Fig. 5a illustrates the schematic diagram of the sensing performance between the sensors embedded with and without

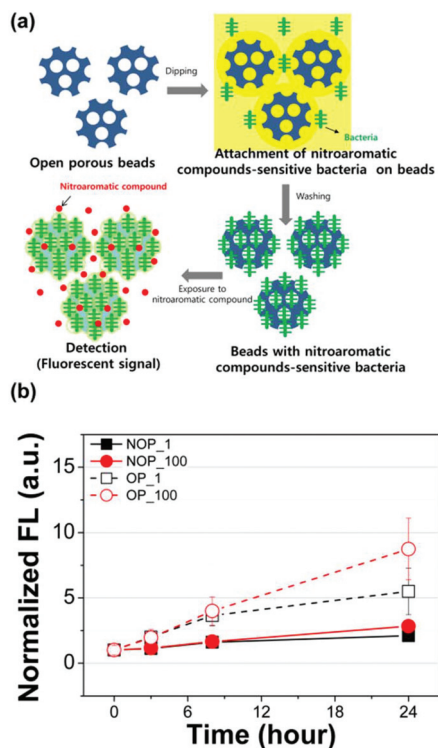


Fig. 3 DNT sensing performance comparison in the non-open porous and open-porous PLGA microbeads. (a) Schematic diagram revealing the application of open-porous microbeads as a nitroaromatic compound detection sensor. (b) The comparison of DNT sensing performance between the non-open porous and porous microbeads.

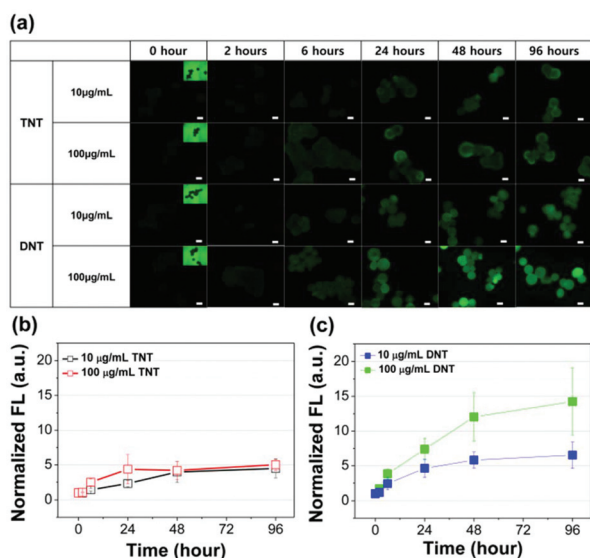


Fig. 4 The sensing performance of the open porous PLGA microbeads in the TNT and DNT solutions. (a) Fluorescence mode OM image of the open porous PLGA microbeads attached with nitroaromatic sensitive bacteria incubating in TNT or DNT solution. Scale bars represent 200  $\mu\text{m}$ . Insets: the OM images of the corresponding images. Normalized fluorescence intensities are shown as a function of the sensing time in the TNT (b) and DNT (c) solutions.

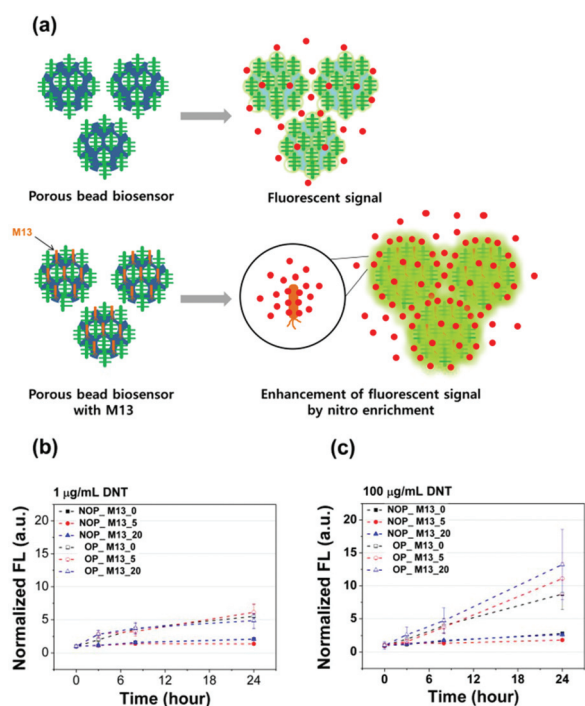


Fig. 5 The enhanced fluorescence intensity as a function of M13 concentration in both non-open porous and open porous microbeads in the DNT solution. (a) The schematic diagram of the enhanced sensing performance embedded with M13 bacteriophages. The normalized fluorescence intensity of M13 embedded sensors in both open porous and non-open porous microbeads in 1  $\mu\text{g mL}^{-1}$  DNT solution (b) and 100  $\mu\text{g mL}^{-1}$  DNT solutions (c).

M13 bacteriophages. The nitroaromatic compound-binding peptide (WHW) was combined on the major coat proteins (pVIII) of the M13 bacteriophages.<sup>41,42</sup> The WHW peptides manifest a remarkable molecular structure to recognize the nitroaromatic compound target. The  $\pi$  electron-rich group of the WHW peptide can bind nitroaromatic compounds through  $\pi$ - $\pi$  interaction.<sup>24,42</sup> Optical microscopy (OM) images in the fluorescence mode of the open porous PLGA microbeads embedded with nitroaromatic-sensitive bacteria and M13 bacteriophage are shown in Fig. S6.† Fig. 5b and c show the normalized fluorescence intensity performance at 1  $\mu\text{g mL}^{-1}$  and 100  $\mu\text{g mL}^{-1}$  DNT solutions, respectively. The non-open porous microbeads cultured without M13 bacteriophage are marked as NOP\_M13\_0 and the open porous microbeads cultured with 5  $\mu\text{g mL}^{-1}$  M13 bacteriophage are marked as OP\_M13\_5. It was confirmed again that the open porous microbeads showed a high normalized fluorescence intensity, regardless of the DNT solution concentration. In Fig. 5c, at the condition of 1  $\mu\text{g mL}^{-1}$  concentration of the DNT solution, the normalized fluorescence intensity is not sensitive to the concentration of the M13 bacteriophage. However, at the condition of 100  $\mu\text{g mL}^{-1}$  DNT concentration, the normalized fluorescence intensities of OP\_M13\_0, OP\_M13\_5 and OP\_M13\_20 were enhanced by 8.7, 11, and 13-folds after 24 hours sensing, respectively. With  $\pi$ - $\pi$  interaction between the M13 bacteriophage and nitroaromatic compound, the DNT molecule was well bound around the nitroaromatic compounds-sensitive bacteria. Moreover, the sensing time was shortened from 96 to 24 hours with the M13 bacteriophage when the normalized fluorescence intensity was enhanced to 14-fold, further resulting in the enhanced sensing behaviour found in the PLGA microbead scaffolds.

## 4. Conclusions

In this study, a bioreporter (green fluorescent bacteria) that can express GFP in response to nitroaromatic compounds was embedded in PLGA biocompatible microbeads as a biosensor. The open porous structure provides permeability and enhances the bioreporter's attachment ability, thereby increasing the expression of the GFP fluorescent signal. Compared with non-open porous microbeads, the fluorescence intensity of the PLGA microbead loading with fluorescent bacteria was increased to a maximum of 1.5 times in the open porous structure microbeads. Based on the sensing mechanism, the fluorescence intensity in the PLGA microbeads loaded with nitroaromatic compounds-sensitive bacteria was increased to a maximum of 5-fold in the TNT groups and 14-fold in the DNT groups, respectively. The durability of the fluorescence signal from this functional microbead sensor could still be detected even after 96 hours. Nitroaromatic compounds-sensitive bacteria with M13 bacteriophages enhanced the normalized fluorescence intensity and decreased the sensing time. Furthermore, the open porous PLGA microbeads loaded with nitroaromatic compounds-sensitive bacteria are expected to be

utilized as a biosensor for the long-distance standoff detection of explosives buried in the soil ground *via* the explosive vapour in a realistic outdoor environment.

## Conflicts of interest

There are no conflicts to declare.

## Acknowledgements

This work was financially supported by the National Research Foundation of Korea Grant funded by the Korean Government (Grants NRF-2021R1A2C2008325 and 2015R1A5A7037615). We thank Prof. Sungkuk Lee at the Ulsan National Institute of Science and Technology for the supply of fluorescent bacteria and nitroaromatic compounds-sensitive bacteria. We thank Prof. Jin-Woo Oh at the Pusan National University for the supply of the M13 bacteriophage. We gratefully acknowledge Prof. Youngkyun Kim at Kookmin University for the use of the fluorescence microscope.

## Notes and references

- 1 P. Kovacic and R. Somanathan, *J. Appl. Toxicol.*, 2014, **34**, 810–824.
- 2 M. Bilal, A. R. Bagheri, P. Bhatt and S. Chen, *J. Environ. Manage.*, 2021, **291**, 112685.
- 3 J. Liu, J. Li, P. Jian and R. Jian, *J. Hazard. Mater.*, 2021, **403**, 123987.
- 4 Z. Mei, H. Qian, D. Liu, Z.-w. YE and C.-x. Lü, *Chin. J. Explos. Propellants*, 2012, **35**, 32–34.
- 5 V. Kumar, N. Choudhury, A. Kumar, P. De and S. Satapathi, *Opt. Mater.*, 2020, **100**, 109710.
- 6 O. Abuzalat, D. Wong, S. S. Park and S. Kim, *Nanoscale*, 2020, **12**, 13523–13530.
- 7 Z. Kayhomayun, K. Ghani and K. Zargoosh, *Mater. Chem. Phys.*, 2020, **247**, 122899.
- 8 O. L. Collin, C. M. Zimmermann and G. P. Jackson, *Int. J. Mass Spectrom.*, 2009, **279**, 93–99.
- 9 G. W. Cook, P. T. LaPuma, G. L. Hook and B. A. Eckenrode, *J. Forensic Sci.*, 2010, **55**, 1582–1591.
- 10 W. Nunes, A. Da Silva, V. Crispim and R. Schirru, *Appl. Radiat. Isot.*, 2002, **56**, 937–943.
- 11 J. I. Steinfeld and J. Wormhoudt, *Annu. Rev. Phys. Chem.*, 1998, **49**, 203–232.
- 12 D. Gao, Z. Wang, B. Liu, L. Ni, M. Wu and Z. Zhang, *Anal. Chem.*, 2008, **80**, 8545–8553.
- 13 H. Turhan, E. Tukenmez, B. Karagoz and N. Bicak, *Talanta*, 2018, **179**, 107–114.
- 14 L. Chen, D. W. McBranch, H.-L. Wang, R. Helgeson, F. Wudl and D. G. Whitten, *Proc. Natl. Acad. Sci. U. S. A.*, 1999, **96**, 12287–12292.
- 15 X. Sun, Y. Wang and Y. Lei, *Chem. Soc. Rev.*, 2015, **44**, 8019–8061.
- 16 H. Zhang, H. Chen, S. Pan, H. Yang, J. Yan and X. Hu, *Luminescence*, 2018, **33**, 196–201.
- 17 X. Xu and Y. Ying, *Food Rev. Int.*, 2011, **27**, 300–329.
- 18 P. Wang, G. Xu, L. Qin, Y. Xu, Y. Li and R. Li, *Sens. Actuators, B*, 2005, **108**, 576–584.
- 19 P. Li, M. Müller, M. W. Chang, M. Frettlöh and H. Schönherr, *ACS Appl. Mater. Interfaces*, 2017, **9**, 22321–22331.
- 20 S. Yagur-Kroll, C. Lalush, R. Rosen, N. Bachar, Y. Moskovitz and S. Belkin, *Appl. Microbiol. Biotechnol.*, 2014, **98**, 885–895.
- 21 S. Yagur-Kroll, E. Amiel, R. Rosen and S. Belkin, *Appl. Microbiol. Biotechnol.*, 2015, **99**, 7177–7188.
- 22 W. G. Miller, J. H. Leveau and S. E. Lindow, *Mol. Plant-Microbe Interact.*, 2000, **13**, 1243–1250.
- 23 K. Lee, S. Choi, C. Kim, W. S. Kang, W. Son, S. C. Bae, J.-W. Oh, S. K. Lee and C. Cha, *ACS Sens.*, 2019, **4**, 2716–2723.
- 24 W.-G. Kim, C. Zueger, C. Kim, W. Wong, V. Devaraj, H.-W. Yoo, S. Hwang, J.-W. Oh and S.-W. Lee, *Org. Biomol. Chem.*, 2019, **17**, 5666–5670.
- 25 T. Qiao, S. Kim, W. Lee and H. Lee, *Macromol. Res.*, 2019, **27**, 321–326.
- 26 E. C. Jensen, *Anat. Rec.*, 2013, **296**, 378–381.
- 27 V. Ljosa and A. E. Carpenter, *PLoS Comput. Biol.*, 2009, **5**(12), e1000603.
- 28 G. A. Van Aken, *Colloids Surf., A*, 2001, **190**, 333–354.
- 29 T. K. Kim, J. J. Yoon, D. S. Lee and T. G. Park, *Biomaterials*, 2006, **27**, 152–159.
- 30 T. I. Croll, A. J. O'Connor, G. W. Stevens and J. J. Cooper-White, *Biomacromolecules*, 2004, **5**, 463–473.
- 31 P. Gentile, V. Chiono, I. Carmagnola and P. V. Hatton, *Int. J. Mol. Sci.*, 2014, **15**, 3640–3659.
- 32 Y. Waeckerle-Men and M. Groettrup, *Adv. Drug Delivery Rev.*, 2005, **57**, 475–482.
- 33 C. M. Murphy, M. G. Haugh and F. J. O'Brien, *Biomaterials*, 2010, **31**, 461–466.
- 34 F. J. O'Brien, B. A. Harley, I. V. Yannas and L. J. Gibson, *Biomaterials*, 2005, **26**, 433–441.
- 35 Y. Lv, Z. Lin and F. Svec, *Anal. Chem.*, 2012, **84**, 8457–8460.
- 36 W. J. Li, C. T. Laurencin, E. J. Caterson, R. S. Tuan and F. K. Ko, *J. Biomed. Mater. Res.*, 2002, **60**, 613–621.
- 37 M. Fletcher and G. Loeb, *Appl. Environ. Microbiol.*, 1979, **37**, 67–72.
- 38 Y.-L. Ong, A. Razatos, G. Georgiou and M. M. Sharma, *Langmuir*, 1999, **15**, 2719–2725.
- 39 R. M. Donlan, *Emerging Infect. Dis.*, 2002, **8**, 881.
- 40 D. Kim, M. Thangavelu, J. S. Baek, H. S. Kim, M. J. Choi, H. H. Cho, J. E. Song and G. Khang, *Macromol. Res.*, 2019, **1–7**.
- 41 W.-J. Chung, J.-W. Oh, K. Kwak, B. Y. Lee, J. Meyer, E. Wang, A. Hexemer and S.-W. Lee, *Nature*, 2011, **478**, 364–368.
- 42 R. A. Blaik, E. Lan, Y. Huang and B. Dunn, *ACS Nano*, 2016, **10**, 324–332.